Multimode Coherent Hybrid States: Ultrafast Investigation of Double Rabi Splitting between Surface Plasmons and Sulforhodamine 101 Dyes

Hai Wang, Hai-Yu Wang, Lei Wang, Qi-Dai Chen, Huai-Liang Xu, Angelica Carrara, Remo Proietti Zaccaria, Hong-Bo Sun,* and Andrea Toma**

A multimode coherent hybrid system formed by strongly coupled surface plasmons in gold nanohole arrays and excitons in sulforhodamine 101 dyes is investigated by using both a steady-state spectroscopic method and a femtosecond transient absorption spectra approach. A double Rabi splitting up to 255 meV and 188 meV is observed in steady-state transmission measurements. Furthermore, the dynamics of the multimode coherent hybrid system are studied under upper band resonant excitation. It is found that the bleaching signal associated with uncoupled sulforhodamine 101 molecules completely disappears. Instead, two distinctive bleaching signals corresponding to the middle and lower bands are formed, thus highlighting the presence of coherent hybrid states. Finally, a remarkebly long lifetime for the lower band is observed, even longer than the bleaching recovery of the uncoupled dyes, in perfect agreement with the non-Markovian regime. These peculiar features can provide new perspectives for coherent energy transfer and mode-selective chemistry, thus enriching the tools available in the chemical reaction landscape.

Molecular photonics is an exponentially growing research area located at the strategic conjunction between nano-optics and quantum electrodynamics where the controlled manipulation of light-matter interaction is currently yearning for the ultimate space- and timescale limits.[1,2] Within this context, organic laser dyes have recently attracted significant attention as optically active media. Owing to their strong oscillator strength and broad tunable emission,[3,4] organic laser dye molecules are the most promising candidates for supporting strong light-matter interaction.[5,6] Strong coupling is achieved when the rate of energy exchange between excitons and light is faster than any of their intrinsic dissipation rates. This gives rise to new coherent hybrid states endowed with unique mixed properties of light and matter.[7–12] As a result, intriguing novel applications are observed, such as quantum information processing,[13] ultrafast switching[14] and thresholdless lasers.[5] In addition, as an attractive subject that has been recently demonstrated, strong coupling can modify the work-function,[15] energy transfer pathways,[16,17] and even conductivity[18] in organic molecules. These functions are normally achieved by placing the organic molecules in a confined electromagnetic (EM) field, such as Fabry–Perot microcavities, which are defined by two metal mirrors working at resonant frequencies.[19] Besides, surface plasmon (SP) modes represent a viable alternative, since they support giant EM field enhancement and therefore strong coupling conditions.[20] In particular, strong coupling has been achieved in hybrid system consisting of plasmonic nanoparticle/nanodisk arrays and Fabry–Perot microcavities.[21,22] Such hybrid systems provide additional interesting pathways for promoting strong coupling with dye molecules.

SPs are light trapped states at the surface of a metal, resulting from their interaction with the free electron gas.[20] In this case, both the light and the matter components can be confined into the nanometer scale, thus envisioning new perspectives for the study of strong coupling at the nanolevel. When strong coupling between SPs and organic molecules is achieved, the excitation energy is shared and oscillates between them (Rabi oscillations), leading to the formation of new hybrid exciton–plasmon states. The energy separation is called Rabi splitting energy and it is defined as $E_R = \hbar\Omega_R$. Based on the rotating-wave approximation,[23] quantum theory predicts that for an individual two-level molecule, the Rabi splitting is given by Equation (1)

Dr. H. Wang, Prof. H.-Y. Wang, Dr. L. Wang, Prof. Q.-D. Chen, Prof. H.-L. Xu, Prof. H.-B. Sun
State Key Laboratory on Integrated Optoelectronics
College of Electronic Science and Engineering
Jilin University
Changchun 130012, China
E-mail: haiyu_wang@jlu.edu.cn; hbsun@jlu.edu.cn

Dr. H. Wang, A. Carrara, Prof. R. Proietti Zaccaria, Dr. A. Toma
Istituto Italiano di Tecnologia
via Morego 30, 16163 Genova, Italy
E-mail: andrea.toma@iit.it

A. Carrara
Università degli Studi di Genova
16145 Genova, Italy

Prof. R. Proietti Zaccaria
Ningbo Institute of Materials Technology and Engineering
Chinese Academy of Sciences
Ningbo 315201, China

DOI: 10.1002/adom.201600857

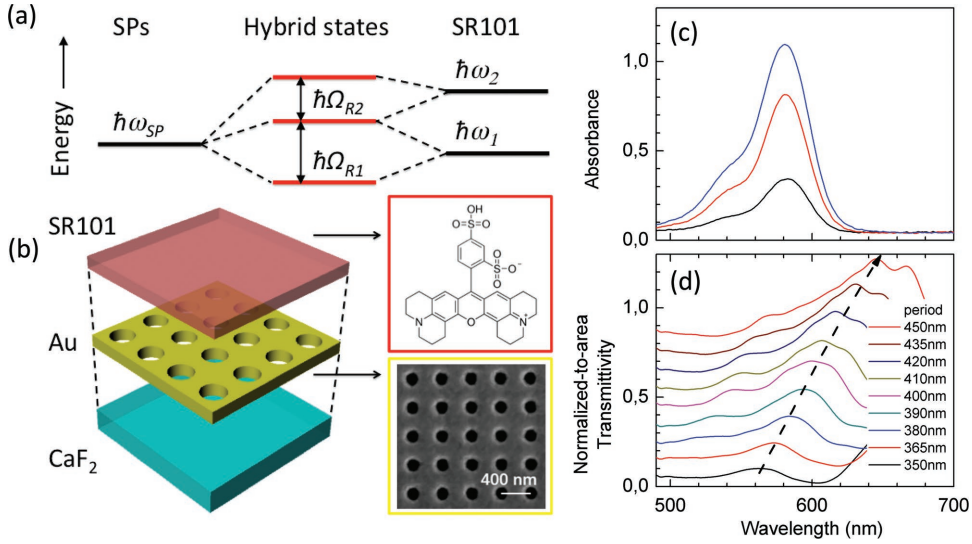

Figure 1. a) The mode diagram of the hybrid exciton–plasmon system is shown, where the middle column depicts the multiple hybrid states observed in strong coupling regime (double Rabi splitting). b) The sample architecture (exploded view) is reported. The red upper part illustrates the chemical structure of sulforhodamine 101 dyes, while a representative SEM image of the Au nanohole array is shown in the yellow box. c) Absorption spectra of sulforhodamine 101 molecules dispersed in SU-8 epoxy-based polymer resist at different concentrations (10, 20 and 30 mg mL^{-1}, black, red, and blue lines, respectively). d) Normalized-to-area transmission spectra for gold nanohole arrays covered with bare SU-8 films. As illustrated, the SP resonance wavelength (black-dashed arrow) was tuned from 566 to 645 nm, while the lattice period was changed from 350 to 450 nm.

$$\hbar\,\Omega_{\mathrm{R}} = 2\sqrt{\frac{\hbar\omega}{2\varepsilon_0 V}}d\sqrt{n_{\mathrm{ph}}+1} \tag{1}$$

where d is the molecular transition dipole moment of the oscillator in the molecule exciton, $\hbar\omega$ is the SPs resonance energy, ε_0 is the vacuum permittivity, V is the mode volume, and n_{ph} refers to the number of photons present in the hybrid system. In addition, when a number N of molecules is considered, the Rabi splitting is proportional to the square root of the density of oscillators (i.e., $\hbar\Omega_{\mathrm{R}} \propto \sqrt{N/V}$).[24]

To date, strong coupling between SPs and organic molecules have been the subject of an intense investigation, in which a huge Rabi splitting up to 780 meV has been observed.[25] Among the many kinds of organic dyes, rhodamine-like molecules are one of the most popular candidates for strong coupling. Since the pioneering work of Cade et al.[26] a giant Rabi splitting of 400 meV has been shown in a monolayer of rhodamine 6G spin-coated on nanostructured Ag films. Concurrently, double vacuum Rabi splitting energies up to 230 and 110 meV with rhodamine 6G have been reported by Hakala et al.[27] In particular, they compared energies and intensities of the in- and out-coupled modes by investigating the system dynamics through reflectometry technique. More recently, strong coupling between SPs and other kinds of rhodamine-like molecules has been demonstrated, for instance with rhodamine 800[28] and sulforhodamine 101.[29] In contrast to the single Rabi splitting, the possibility to induce multimode coherent hybrid states can envision interesting perspective for a better comprehension of the strong coupling dynamics, such as the energy transfer between multiple exciton-SPP branches.[27] Moreover, the investigation of complex multimode states can reveal new possibilities in the context of mode-selective chemistry, thus enriching the available tools for modifying the chemical reaction landscape.[30]

In this letter, we explore the ultrafast dynamics of strongly coupled hybrid-states involving a gold nanohole array and a sulforhodamine 101 (SR101) dye. A double Rabi splitting was observed in steady-state transmission measurements, while the dynamics of the multimode hybridization under double splitting was studied by transient absorption (TA) microscopy. In particular, due the presence of two excitons, the investigation of the middle branch dynamics appears extremely interesting since it presents plasmon-induced hybridization between the two SR101 excitons.[27]

The scheme of the samples used in this work is shown in **Figure 1**. The investigated hybrid systems consist of a 200 nm thick Au film, which has been patterned by means of focused ion beam (FIB) to create a 2D square lattice gold nanohole array (see Figure 1b). Three different samples have been prepared by spin-coating a uniform layer (300 nm thick) of SR101/SU-8 films with different concentrations (more details are given in the Experimental Section). In order to determine the absorbance of the SR101/SU-8 films, samples without gold layer were fabricated. The corresponding absorbance spectra, which have a main and shoulder peak at around 580 and 540 nm, are shown in Figure 1c. The absorbance values of SR101/SU-8 films at 580 nm are 0.34, 0.81 and 1.10, respectively.

Figure 1d shows the transmission spectra recorded for different gold nanohole arrays covered with bare SU-8 films. As illustrated, the SP resonance wavelength (pronounced peaks in Figure 1d) was tuned from 566 nm to 645 nm, while the lattice period was changed from 350 nm to 450 nm. Normal incidence transmission spectra for a series of hybrid systems with different SR101 concentration are shown in **Figure 2**a–c. For each concentration, three peaks appear and redshift with the lattice

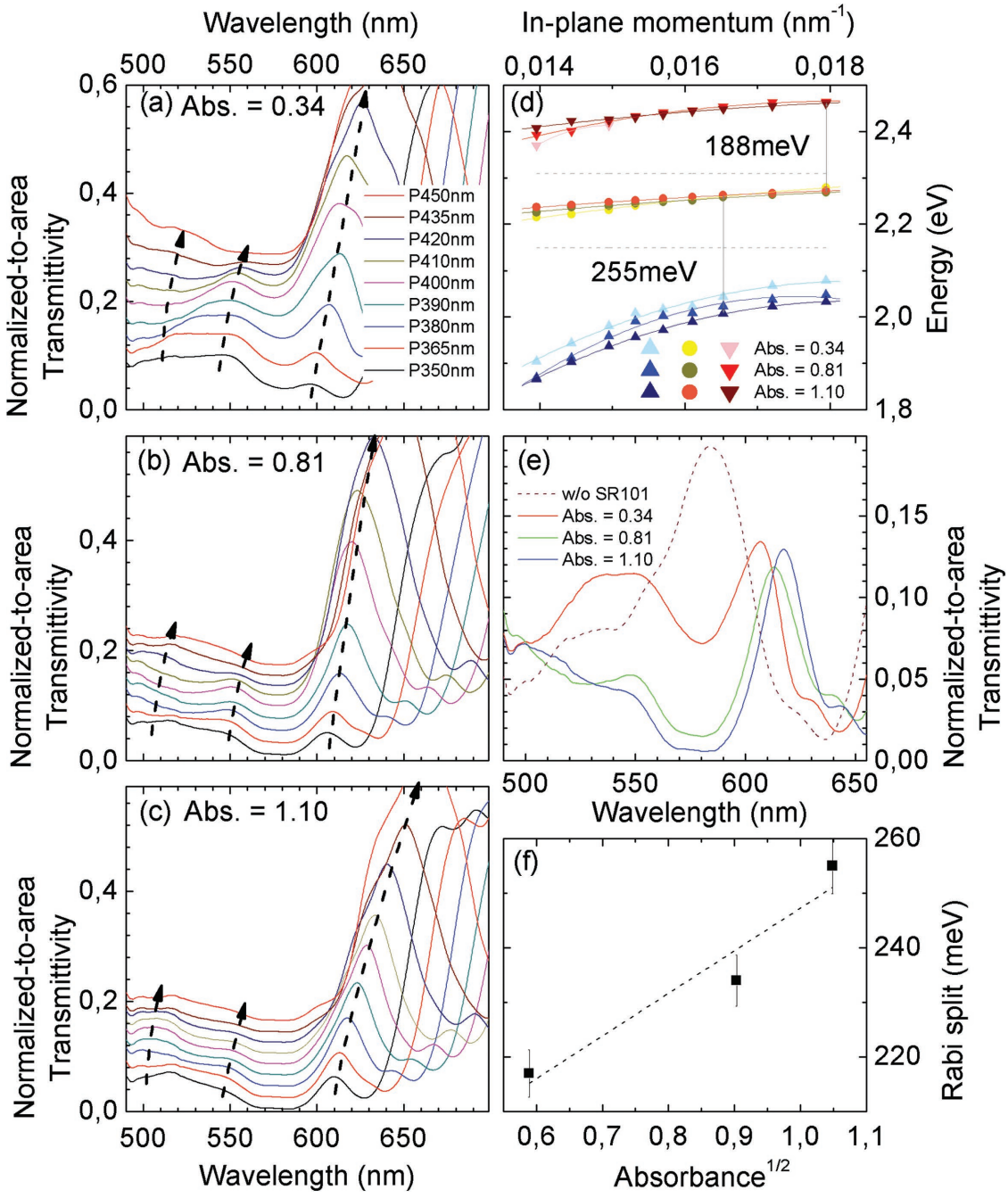

Figure 2. Transmission spectra normalized to the area occupied by the holes have been acquired for a series of hybrid systems with different SR101 concentrations: a) 10, b) 20, and c) 30 mg mL^{-1}. In every case, three peaks appear and redshift by increasing the lattice period from 350 to 450 nm. The energy dispersion curves are summarized in (d), where the three bands measured by changing the SR101 concentration are highlighted. The normalized-to-area transmission spectra acquired for resonance period 380 nm and different concentrations are compared in (e). By increasing the SR101/SU-8 absorbance, the Rabi splitting between the lower and middle bands varies from 217 to 255 meV. f) Experimental Rabi splitting values as a function of the square root of the SR101/SU8 film absorbance.

period increasing. Compared to Figure 1d, the transmission spectra of the whole system are significantly modified, thus highlighting the formation of novel exciton–plasmon hybrid states.

The upper and lower bands are originating from the coupling between the SPs and the excitons, which correspond to the main and shoulder SR101 absorption peaks, respectively. On the contrary, the middle band presents hybridization between SPs and both SR101 excitonic modes (as schematically sketched in Figure 1a). It is worth to be noticed that when the gold nanohole period equals 380 nm, the SP resonance matches the main absorption of SR101, thus maximizing the

coupling strength. Conversely, the plasmon mode with 350 nm periodicity matches the shoulder absorption of SR101. Hence, a double Rabi splitting is expected and observed for the two resonant periods.

The dispersion curves of the three bands measured by changing the SR101 concentration are summarized in Figure 2d. An anticrossing behavior is clearly observed, as expected for the strong coupling regime.[31] By increasing the SR101 concentration the Rabi splitting widens in accordance to $\hbar\Omega_R \propto \sqrt{N/V}$. The measured double Rabi splitting energies for the highest concentration sample are 255 meV and 188 meV, respectively. The normalized-to-area transmission spectra acquired for resonance period 380 nm and different concentrations were compared in Figure 2e. In particular, the brown dashed line represents the optical behavior of the gold nanohole array covered by 300 nm thick SU-8 film in absence of SR101 dyes. The SPP resonance supported by the system is clearly highlighted. By increasing the SR101/SU-8 film absorbance, the Rabi splitting between the lower and middle bands varies from 217 meV to 255 meV, following a linear dependence on the square root of SR101 absorbance (see Figure 2f). This behavior is consistent with previous experimental results and quantum theory description on strongly coupled hybrid systems.[31] To gain further insight into the photophysical nature of such hybrid system, TA spectroscopy experiments were carried out.

Femtosecond TA spectra were carried out with a 100 fs laser pump-probe setup.[32,33] The reference sample with SR101/SU-8 spin-coated on flat gold film was pumped by a 500 nm laser pulse. In order to reduce the molecule aggregation probability, the sample with the lowest concentration was chosen. As shown in **Figure 3**a, the TA spectra are dominated by a negative signal with a main and shoulder peak at 593 and 570 nm, respectively. The observed features appear redshifted with respect to the steady-state peaks. This can be assigned to the overlap between the stimulated emission (SE) from the excited state and the SR101 ground state bleaching signal. The wide negative signal from 640 nm to 730 nm can also be ascribed to the weak SE of the SR101 molecules.[34]

TA experiments have been performed on the hybrid system, keeping the SR101 concentration equal to the reference case. The sample was resonantly pumped at 500 nm in correspondence of the upper hybrid band. Totally different TA features emerged from the hybrid system if compared with the reference one. As shown in Figure 3b, the two bleaching signals at 566 and 614 nm can be assigned to the lower and middle hybrid bands, in good agreement with the steady-state transmission measurements. It is worth noticing the presence of a shoulder peak in the lower band, which can be ascribed to the SE from the same band. Unfortunately, the upper band dynamics cannot be investigated, due to the aforementioned limitations in the detection window. However, particular attention should be paid to the fact that no positive signals have been recorded: a behavior related to the absence of any thermal effect.[35] In this view, multimode coherent hybrid systems appear to be the most promising candidates for the direct investigation of SP-related nonthermal dynamics.

The kinetics process associated to the middle and lower hybrid bands are illustrated in Figure 3c. By a first look of the

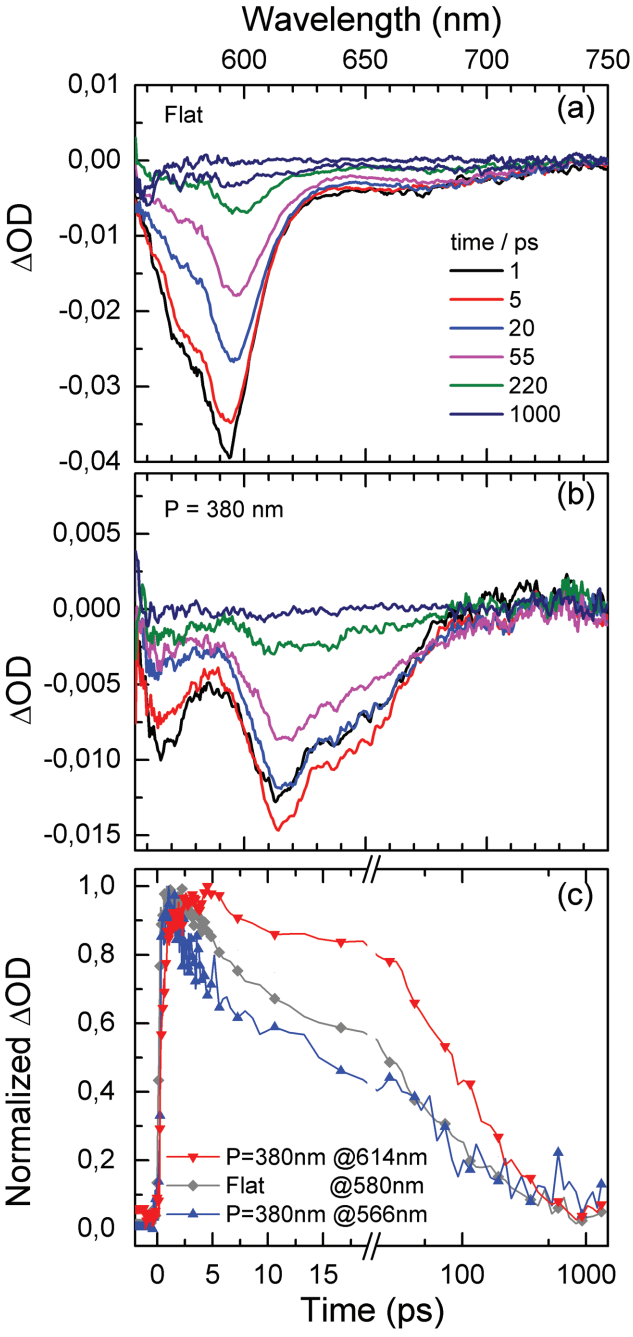

Figure 3. Transient absorption spectra of a) SR101 on flat gold film and b) SR101 on nanohole array with periodicity 380 nm (i.e., overlapping condition for sulforhodamine 101 molecules and SPs absorption peaks in static regime). Resonant excitation in correspondence of the upper hybrid band (500 nm) has been employed. The normalized bleaching dynamics of the middle and lower hybrid bands is summarized in (c). ΔOD: optical density variation.

TA spectra, we can immediately recognize that the lower band possesses a slower lifetime, while the middle band a faster decay, if compared with the ground state bleaching dynamics of the SR101 on flat gold film. However, since the lower and middle bands both consist of strongly coupled SPs and SR101 excitons coming from the main absorption peak at 580 nm, it

should be stressed that, in the bleaching dynamics, the lower and the middle bands are sharing a common ground state. Hence, it is not straightforward to precisely identify in which excited state (middle or lower) the hybrid system is located. Moreover, no accurate predictions can be done on the decay times of the two hybrid states. Nevertheless, we found that the middle band shows a fast decay at the early stages (blue triangles in Figure 3c), while the lower band displays a slow initial rise (red circles in Figure 3c). This behavior can be ascribed to a relaxation of the middle band into the lower band population. Namely, the lower band can be thought as a potential-minimum quasi-bound state. This is in agreement with previous reports:[36] the lifetime of the lower hybrid band is longer than the bleaching recovery of SR101 molecules. In fact, the observed experimental lifetimes of the hybrid states correspond well with a non-Markovian regime.[37] In such a case, the lifetime of the lower band can be relatively long and always presents a much slower decay in comparison to the middle/upper band.

In summary, we have experimentally demonstrated the strong coupling between excitons in SR101 molecules and SPs in gold nanohole arrays. A double Rabi splitting has been observed up to 255 and 188 meV. The dispersion of the exciton–plasmon hybrid states is in excellent agreement with the typical signature of strong coupling, i.e., anticrossing behavior. Moreover, we verified that the energies of the observed Rabi splitting depend on the square root of the SR101 molecule absorbance. Both the evidences confirmed that the interaction between SPs and SR101 molecules was in the strong coupling regime. The dynamics of the multimode hybrid states has been studied by TA spectroscopy under upper band resonant excitation. In the TA spectra the bleaching signal coming from the uncoupled SR101 is completely absent; instead, two distinctive bleaching signals corresponding to the middle and lower bands have been observed, thus confirming the formation of coherent hybrid states. Finally, by a deeper analysis of the ultrafast kinetics, an effective relaxation from the middle to the lower bands was found. Due to the large Rabi splitting, the lifetime of the lower band can be intrinsically longer than the bleaching recovery of the uncoupled dyes, in perfect agreement with the non-Markovian regime. Such an understanding on the dynamics of multimode coherent hybrid systems, involving broad absorption dye molecules, is of fundamental importance for its implications in low-threshold lasing and room temperature Bose–Einstein condensation.[6,38]

Experimental Section

Sample Fabrication: To fabricate the sample, 200 nm of gold was deposited on CaF_2(100) substrate by electron beam evaporation. Then, 2D square lattice gold nanohole arrays with different diameters and periodicities were fabricated via FIB lithography. The lattice period varied from 350 to 450 nm, while the ratio of the period-to-diameter was kept constant at 2.5. Each individual array was 60×60 μm^2 large. Three different samples were prepared by spin-coating a uniform layer (300 nm thick) of SR101/SU-8 films on top of the gold nanohole arrays. The molecule/polymer layer was completely filling the subwavelength holes. In details, sulforhodamine 101 molecules were dispersed in SU-8 epoxy-based polymer resist (Microchem SU-8 2025) by changing their concentration (10, 20, and 30 mg mL^{-1}). In order to prevent oxidization, the samples were sealed by a glass slide under nitrogen environment in a glove box with oxygen concentration smaller than 0.1 ppm.

Transient Absorption Measurements: Femtosecond TA spectra were recorded with a 100 fs laser pump-probe setup. A mode-locked Ti:sapphire laser/amplifier system (Solstice, Spectra-Physics) was used. The amplified output from the regenerative amplifier (RGA, Spitfire, Spectra Physics) at a 250 Hz repetition rate with pulse energy of 1.5 mJ, 100 fs pulse width, and 800 nm wavelength was split into two parts. The stronger part was used to generate the desired excitation pulse at $\lambda = 500$ nm through the TOPAS system; the other part was focused on a sapphire substrate to generate a broadband white light (from 450 to 800 nm) as probe pulse. The two beams were orthogonally collinearly recombined by a dichroic mirror and then, through a microscope objective (NA 0.75, magnification 10), focused on the sample at normal incidence. It is worth noting that, due to chromatic aberrations, the focal planes of the pump and probe beams were different. In the present experiments, it was decided to optimize the probe beam focusing. Conversely, the pump would be out of focus, thus providing a spatially uniform excitation pulse larger than the probed area. The reflected light from the sample was collected through the same objective. Finally, blocking the excitation light by a proper filter, the TA data were acquired by a fiber-coupled sensitive spectrometer (Avantes AvaSpec-2048×14) in the detection window ranging from 560 to 800 nm (a dichroic mirror was limiting the probe light). The group velocity dispersion of the transient spectra was compensated by a chirp program.

Acknowledgements

The authors would like to recognize the financial support from the National Science Foundation (Award Nos. 1102301 and 1254934), from the National Basic Research Program of China (973 Program, Grant No. 2014CB921300), Natural Science Foundation China (NSFC) under Grant Nos. 21273096 and 21473077 and from the Doctoral Fund Ministry of Education of China under Grant No. 20130061110048.

Received: October 17, 2016
Revised: January 11, 2017
Published online: March 21, 2017

[1] J. H. Burroughes, D. D. C. Bradley, A. R. Brown, R. N. Marks, K. Mackay, R. H. Friend, P. L. Burns, A. B. Holmes, *Nature* **1990**, *347*, 539.
[2] G. Li, R. Zhu, Y. Yang, *Nat. Photonics* **2012**, *6*, 153.
[3] I. D. W. Samuel, G. A. Turnbull, *Chem. Rev.* **2007**, *107*, 1272.
[4] G. Kranzelbinder, G. Leising, *Rep. Prog. Phys.* **2000**, *63*, 729.
[5] M. A. Noginov, G. Zhu, A. M. Belgrave, R. Bakker, V. M. Shalaev, E. E. Narimanov, S. Stout, E. Herz, T. Suteewong, U. Wiesner, *Nature* **2009**, *460*, 1110.
[6] P. Berini, I. De Leon, *Nat. Photonics* **2012**, *6*, 16.
[7] Y.-W. Hao, H.-Y. Wang, Y. Jiang, Q.-D. Chen, K. Ueno, W.-Q. Wang, H. Misawa, H.-B. Sun, *Angew. Chem.* **2011**, *123*, 7970.
[8] Z.-Y. Zhang, H.-Y. Wang, J.-L. Du, X.-L. Zhang, Y.-W. Hao, Q.-D. Chen, H.-B. Sun, *Appl. Phys. Lett.* **2014**, *105*, 191117.
[9] H. Wang, A. Toma, H.-Y. Wang, A. Bozzola, E. Miele, A. Haddadpour, G. Veronis, F. De Angelis, L. Wang, Q.-D. Chen, H.-L. Xu, H.-B. Sun, R. P. Zaccaria, *Nanoscale* **2016**, *8*, 13445.
[10] D. G. Lidzey, D. D. C. Bradley, M. S. Skolnick, T. Virgili, S. Walker, D. M. Whittaker, *Nature* **1998**, *395*, 53.
[11] H. Wang, H.-Y. Wang, A. Bozzola, A. Toma, S. Panaro, W. Raja, A. Alabastri, L. Wang, Q.-D. Chen, H.-L. Xu, F. De Angelis, H.-B. Sun, R. P. Zaccaria, *Adv. Funct. Mater.* **2016**, *26*, 6198.
[12] P. Törmä, W. L. Barnes, *Rep. Prog. Phys.* **2015**, *78*, 013901.
[13] G. Kurizki, P. Bertet, Y. Kubo, K. Mølmer, D. Petrosyan, P. Rabl, J. Schmiedmayer, *Proc. Natl. Acad. Sci.* **2015**, *112*, 3866.

[14] T. Ming, L. Zhao, M. Xiao, J. Wang, *Small* **2010**, *6*, 2514.
[15] J. A. Hutchison, A. Liscio, T. Schwartz, A. Canaguier-Durand, C. Genet, V. Palermo, P. Samorì, T. W. Ebbesen, *Adv. Mater.* **2013**, *25*, 2481.
[16] S. Balci, C. Kocabas, B. Küçüköz, A. Karatay, E. Akhüseyin, H. Gul Yaglioglu, A. Elmali, *Appl. Phys. Lett.* **2014**, *105*, 051105.
[17] D. M. Coles, N. Somaschi, P. Michetti, C. Clark, P. G. Lagoudakis, P. G. Savvidis, D. G. Lidzey, *Nat. Mater.* **2014**, *13*, 712.
[18] E. Orgiu, J. George, J. A. Hutchison, E. Devaux, J. F. Dayen, B. Doudin, F. Stellacci, C. Genet, J. Schachenmayer, C. Genes, G. Pupillo, P. Samori, T. W. Ebbesen, *Nat. Mater.* **2015**, *14*, 1123.
[19] A. Kavokin, J. J. Baumberg, G. Malpuech, F. P. Laussy, *Microcavities*, Oxford University Press, Oxford, UK **2007**.
[20] W. L. Barnes, A. Dereux, T. W. Ebbesen, *Nature* **2003**, *424*, 824.
[21] S. Chen, G. Li, D. Lei, K. W. Cheah, *Nanoscale* **2013**, *5*, 9129.
[22] M. A. Schmidt, D. Y. Lei, L. Wondraczek, V. Nazabal, S. A. Maier, *Nat. Commun.* **2012**, *3*, 1108.
[23] E. T. Jaynes, F. W. Cummings, *Proc. IEEE* **1963**, *51*, 89.
[24] R. J. Thompson, G. Rempe, H. J. Kimble, *Phys. Rev. Lett.* **1992**, *68*, 1132.
[25] A. Cacciola, O. Di Stefano, R. Stassi, R. Saija, S. Savasta, *ACS Nano* **2014**, *8*, 11483.
[26] N. I. Cade, T. Ritman-Meer, D. Richards, *Phys. Rev. B* **2009**, *79*, 241404.
[27] T. K. Hakala, J. J. Toppari, A. Kuzyk, M. Pettersson, H. Tikkanen, H. Kunttu, P. Törmä, *Phys. Rev. Lett.* **2009**, *103*, 053602.
[28] F. Valmorra, M. Bröll, S. Schwaiger, N. Welzel, D. Heitmann, S. Mendach, *Appl. Phys. Lett.* **2011**, *99*, 051110.
[29] S. Baieva, T. Hakala, J. Toppari, *Nanoscale Res. Lett.* **2012**, *7*, 1.
[30] J. A. Hutchison, T. Schwartz, C. Genet, E. Devaux, T. W. Ebbesen, *Angew. Chem., Int. Ed.* **2012**, *51*, 1592.
[31] J. Dintinger, S. Klein, F. Bustos, W. L. Barnes, T. W. Ebbesen, *Phys. Rev. B* **2005**, *71*, 035424.
[32] H. Wang, H.-Y. Wang, B.-R. Gao, Y. Jiang, Z.-Y. Yang, Y.-W. Hao, Q.-D. Chen, X.-B. Du, H.-B. Sun, *Appl. Phys. Lett.* **2011**, *98*, 251501.
[33] L. Wang, Q. Li, H.-Y. Wang, J.-C. Huang, R. Zhang, Q.-D. Chen, H.-L. Xu, W. Han, Z.-Z. Shao, H.-B. Sun, *Light: Sci. Appl.* **2015**, *4*, e245.
[34] M. Fedoseeva, R. Letrun, E. Vauthey, *J. Phys. Chem. B* **2014**, *118*, 5184.
[35] N. J. Halas, S. Lal, W.-S. Chang, S. Link, P. Nordlander, *Chem. Rev.* **2011**, *111*, 3913.
[36] T. Schwartz, J. A. Hutchison, J. Léonard, C. Genet, S. Haacke, T. W. Ebbesen, *ChemPhysChem* **2013**, *14*, 125.
[37] A. Canaguier-Durand, C. Genet, A. Lambrecht, W. T. Ebbesen, S. Reynaud, *Eur. Phys. J. D* **2015**, *69*, 1.
[38] J. D. Plumhof, T. Stöferle, L. Mai, U. Scherf, R. F. Mahrt, *Nat. Mater.* **2014**, *13*, 247.